ChemistrySelect

Supporting Information

Layer by Layer Deposition of 1T′-MoS_2 for the Hydrogen Evolution Reaction

Farbod Alimohammadi, Parisa Yasini, Tim Marshall, Nuwan H. Attanayake, Eric Borguet, and Daniel R. Strongin*

Experimental Section

Chemicals:

Sulfuric acid (H_2SO_4, 98%) was obtained from Fisher Chemical. Aniline (≥99.5%), n-butyllithium (n-Butyllithium solution, 1.6 M in hexane), and molybdenum (IV) sulfide were purchased from Sigma-Aldrich. All chemicals were used as received without further purification. Deionized (DI) water was provided by an in-house Thermoscientific Barnstead Easypure II purification system equipped with a UV lamp (water resistivity >18 MΩ.cm).

Preparation of MoS_2:

1T'-MoS_2 was prepared by Li-intercalation of bulk MoS_2 which involved treating the metal dichalcogenide with 1.6 M n-butyl lithium (n-BuLi) in 10 mL of hexane under an argon atmosphere for 48 h.[1] The Li-MoS_2 (Li_xMoS_2) was filtered and washed with excess hexane to remove residual lithium and organic material. The sample was then dried under vacuum at room temperature for 48 hours. The Li-MoS_2 sample was exfoliated by sonicating 0.10 g of the material in 40 ml of DI water for one hour. The resulting material was centrifuged and washed to eliminate any unexfoliated MoS_2 and LiOH. This procedure provided a solution with a 1T'-MoS_2 loading of 2 mg/ml. X-ray photoelectron spectroscopy (XPS) and STM characterization of the MoS_2 sheets are presented in the supporting information (**Figure S1-S2**). 2H-MoS_2 flakes were grown by chemical vapor deposition (CVD) with solid MoO_3 and S precursors on a HOPG substrate for the STS measurements.

Preparation of LbL films of 1T'-MoS_2 and 2H-MoS_2:

1T'-MoS_2 layers were assembled by the LbL method on three different substrates: FTO coated glass, a thin Au(111) overlayer on mica, and highly oriented pyrolytic graphite (HOPG). With regard to FTO, coated glass pieces (1×2 cm) of the material were cleaned by ultrasonic washing in acetone, ethanol, and water. The assembly procedure was started by exposing (dip-coated for 5 min) the FTO surface into a solution of polyaniline (PANI) to create a positively charged layer on the FTO surface to electrostatically bind the first deposited layer of negatively charged MoS_2.[2] PANI was synthesized by a previously reported procedure.[3] In brief, 1.4 ml of aniline (0.15 M) was dissolved in 0.1 M HCl (100 ml). A 40 ml ferric chloride solution (50 g/L) was added dropwise into the aniline solution. The resulting polyaniline was collected by centrifugation, and washed with 1 M HCl, 1 M NH_3, N-Methyl-2-pyrrolidone, and methanol. Infrared spectroscopy was used to confirm the formation of PANI (**Figure S3**).

Deposition of MoS_2 layers on Au(111) was carried out without the use of a transition layer (i.e., PANI). The PANI layer was not needed presumably due to the strong interaction of the S component of MoS_2 with gold. Subsequent assembly of MoS_2 layers was carried out by utilizing two solutions: a 1T'-MoS_2 solution with a loading of 0.5 mg/ml

and a 10 mM sodium chloride solution. A single initial cycle (i.e., cycle 1) consisted of 1) dipping the PANI coated FTO in the 1T'-MoS_2 solution for 1 min, 2) dipping the resulting MoS_2/FTO material in DI water, and 3) then dipping the DI washed MoS_2/FTO in the NaCl solution for 1 min and rinsing with DI water. Additional cycles, if desired, were carried out by repeating steps 1 – 3 (Schematic 1).

The conversion of the 1T'-MoS_2 into the 2H-MoS_2 phase on FTO (for electrochemical measurements) or HOPG (for STM measurement) was carried out by individually exposing the 1T'-MoS_2 samples to continuous laser 532 nm light (Coherent Verdi V5). The laser spot had a 4.5 mm diameter at a power of 4.5 W with the 5 minutes exposure time for each spot. The sample was partitioned into several 4x4 mm^2 sections and each section was exposed to the laser for 2.5 minutes. An XY micrometer translational stage was used to move the sample orthogonally to the laser beam to ensure uniform laser exposure across all sections. The mass of the MoS_2 layer(s) assembled on electrodes (FTO) was determined by exposing the electrode to nitric acid (70%) for three days and then analyzing the digested sample with an ICP-MS (Agilent 7900 ICP-MS).[4]

Scanning tunneling microscopy:

A 1T'-MoS_2 suspension was drop-cast on HOPG for STM measurements. HOPG (grade ZYB) was purchased from Bruker and treated with UV/ozone (PSD-UVT from NOVASCAN company) for 5 minutes prior to the deposition of MoS_2. The STM imaging was performed with an Agilent 4500 (Molecular Imaging) microscope under ambient conditions using a mechanically cut Pt-Ir (9:1) wire (diameter 0.25 mm) as an STM tip. All imaging experiments were performed in constant current mode at 300 mV bias voltage. Gwyddion software[5] was used for visualization and analysis of data produced by scanning probe microscopy techniques.

Atomic force microscopy:

Au(111) on mica (Phasis company) was used as the substrate to study the layer by layer formation of MoS_2 sheets by AFM. In order to produce flat, contaminant-free Au (111) surfaces, the substrate was annealed in a hydrogen flame for 2 minutes, followed by immediate quenching in hydrogen-saturated ultraclean water. Three different spots of the sample surface were probed by AFM for the further image analysis (2.5 × 2.5 μm^2). AFM image analysis of assembled MoS_2 on the gold substrate was carried out using Gwyddion software.[5] The surface coverage of the sheets having diameters greater than 50 nm (surface area higher than ~ 0.002 μm^2) was measured, and the surface coverage of three images were used to calculate the standard deviation. AFM imaging was performed with Agilent 5100 microscopes in ambient conditions in tapping mode with conical tips with an aluminum reflex coating (MikroMasch (radius < 8 nm, spring constant = 5 N/m, resonant frequency = 160 kHz)). The roughness average (R_a) was calculated by

Equation 1. r_j represents the vertical distance (height) from the mean value to the j^{th} data point.

$$\mathbf{R_a} = \frac{1}{N}\sum_{j=1}^{N}|r_j| \qquad \textbf{(1)}$$

Raman spectroscopy:

Raman measurements were performed using a Horiba Labram HR800 Evolution confocal Raman spectrometer with an Olympus MPLN100x objective and 1600 gr/mm grating. An excitation wavelength of 532 nm was used, and two accumulations were obtained per spectrum using an integration time of 100 s. Bulk 1T'-MoS_2 drop-cast on sapphire, and the few layer MoS_2 assembled on the FTO were characterized with Raman spectroscopy.

Electrochemistry:

Electrochemical measurements were performed at room temperature using a CH instrument electrochemical analyzer (model CHI604E). A saturated calomel electrode (SCE) served as the reference electrode, graphite was used as the counter electrode, and FTO (1cm×1cm) was used as the working electrode. Linear sweep voltammetry (LSV) measurements were carried out in a 0.5 M H_2SO_4 electrolyte solution. The scan rate used for the LSV was 10 mV/s. The LSV polarization data obtained for 1T' and 2H-MoS_2 (after laser transformation) at a given layer number were collected from the same electrode. The potential was measured relative to the saturated calomel reference electrode (SCE) and then converted to the potential versus the reversible hydrogen electrode (RHE) using the relationship, $E_{RHE} = E_{SCE} + E^0{}_{SCE} + 0.059$ pH. To obtain Tafel plots to evaluate the HER kinetic parameters of the samples, the polarization curves were replotted as overpotential (η) versus log current density (log j):

$$\boldsymbol{\eta = \rho\ \mathrm{Log}\ j + \mathrm{Log}\ j_0} \qquad \textbf{(2)}$$

where j is the current density and ρ is the Tafel slope. Some LSV data presented in this contribution were normalized to the mass of the MoS_2 electrocatalyst on the FTO. This was accomplished by using data from the ICP-MS technique which allowed the determination of the mass and the composition of the MoS_2 electrocatalyst (the polarization curve and mass loading were measured on the same electrode).

Impedance spectroscopy data was obtained at an applied potential of -0.7 V_{SCE} over the frequency range from 5 MHz to 5 mHz. The equivalent circuit for the impedance spectroscopy is presented in **Figure S4**. The polarization curves were replicated at least two times.

X-ray photoelectron spectroscopy

X-ray photoelectron spectroscopy (XPS) measurements were carried out using a conventional laboratory X-ray source (magnesium X-ray source and a 100 mm hemispherical electron energy analyzer) to confirm the phase transition of 2H to 1T' as a result of exfoliation. XPS data for MoS_2 before and after exfoliation are presented in Figures S1. The Mo 3d spectral region of MoS_2 prior to exfoliation exhibits two primary peaks at 229 and 232 eV which are attributed to the $3d_{3/2}$ and $3d_{5/2}$ component of Mo^{4+}, respectively, in agreement with prior studies.[6] XPS analysis of MoS_2 after exfoliation exhibits a broadening of the Mo 3d region. The fitted Mo 3d region exhibits the same 2H features with a reduced spectral area (relative to pre-exfoliated data) as well as new Mo 3d features. The fitted Mo 3d region has greater spectral weight, and the Mo 3d features are shifted to lower binding energy compared to the respective Mo 3d peaks for 2H-MoS_2. These features are associated with the 1T' phase of MoS_2, consistent with prior XPS studies.[6]

Scanning probe microscopy:

Atomic force microscopy (AFM) of layered MoS_2 was carried out on HOPG and Au(111) on mica. Scanning tunneling microscopy imaging was performed with an Agilent 4500 (Molecular Imaging) microscope in ambient condition at room temperature using a mechanically cut Pt-Ir (9:1) wire (diameter 0.25 mm) as an STM tip. STM images confirm the formation of the monolayer 1T'-MoS_2 using the chemical exfoliation method. Although the results of the STM investigation and the synthesis of a superstructure of 1T' MoS_2 by oxidation of intercalated K (H_2O) MoS_2 compound were previously reported, the morphology of the sheets and the I-V curves of 1T'-MoS_2 have not been studied.[7] STM imaging of MoS_2 deposited on HOPG (Figure S2) exhibited monolayers with a height of 0.8 nm, consistent with previously reported MoS_2 layer thicknesses (0.6-0.8 nm).[8] The observed roughness of the edges could be due to experimental set-up in ambient condition, and adsorption of impurities that and bonding to dangling bonds of edge Mo and S atoms.[9]

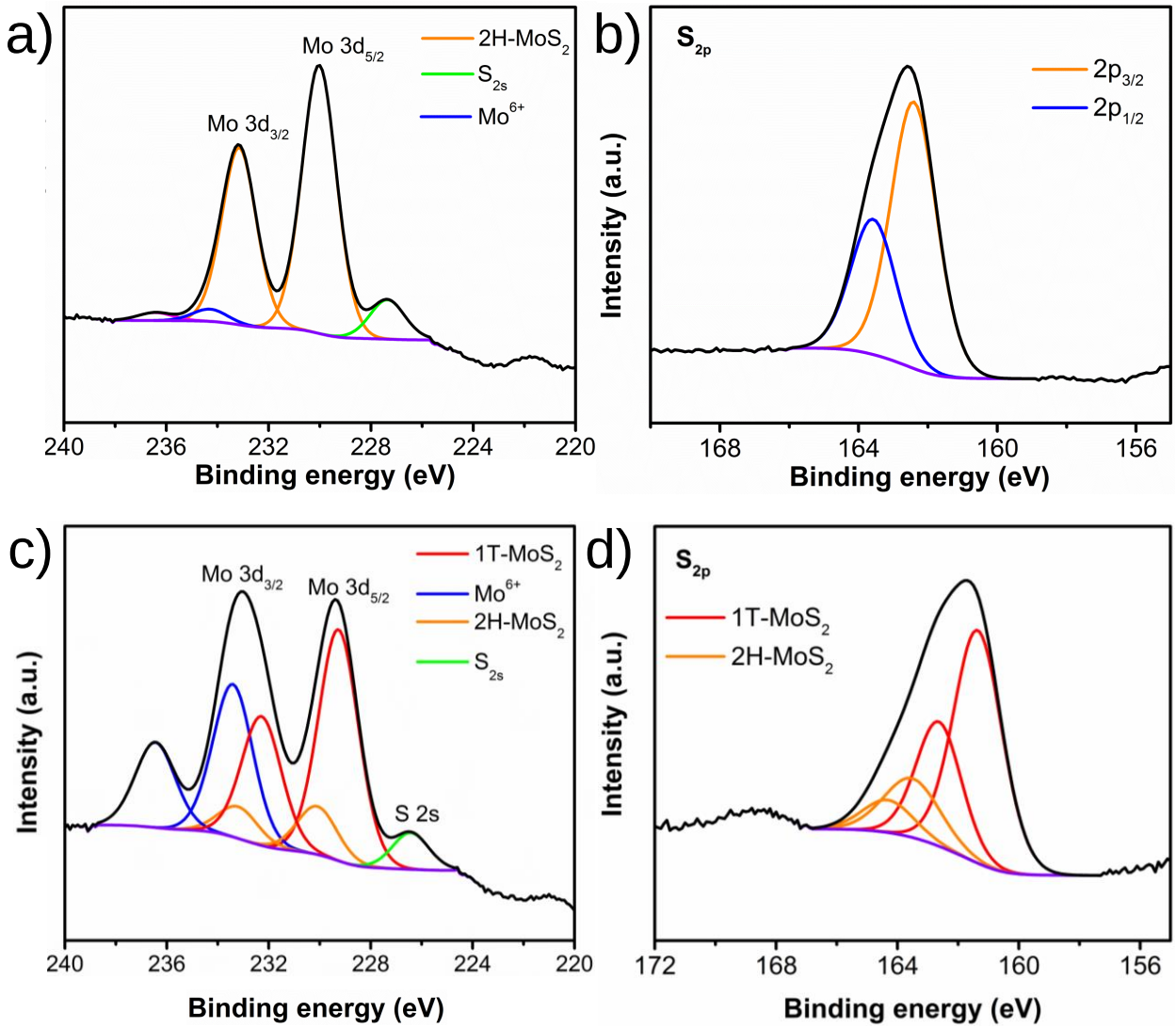

Figure S1. XPS of 2H-MoS_2 for the a) Mo 3d and b) S 2p (fitted $3d_{5/3}$ and $3d_{3/2}$ of Mo and $2p_{3/2}$ and $2p_{1/2}$ of S) features. XPS of MoS_2 after exfoliation, c) the Mo 3d and d) S 2p (fitted $3d_{5/3}$ and $3d_{3/2}$ of Mo and $2p_{3/2}$ and $2p_{1/2}$ of S) spectral features.

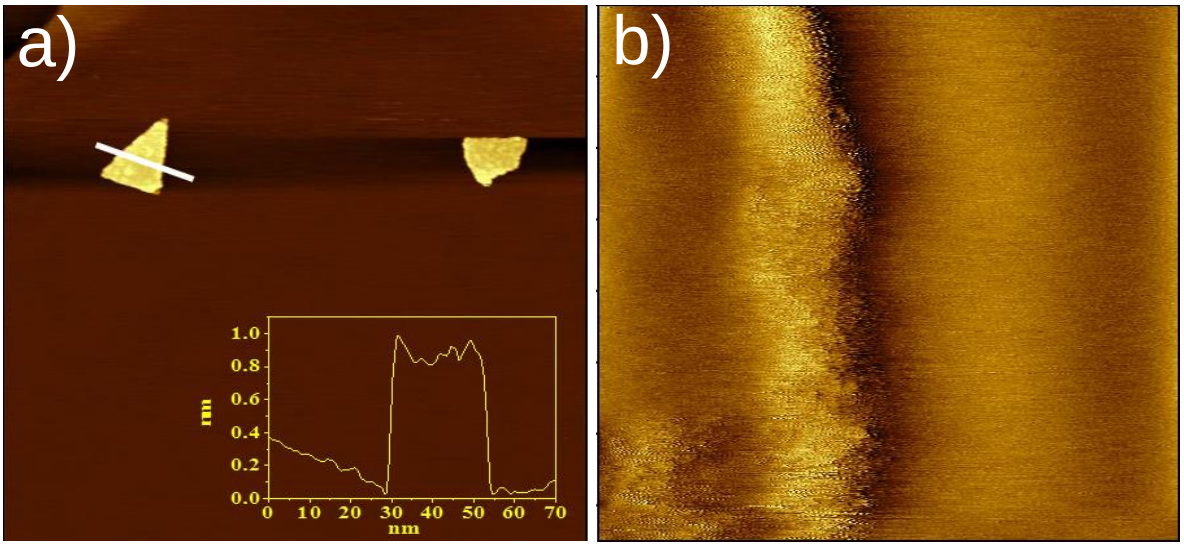

Figure S2. a) STM topography image $(0.25 \times 0.25\ \mu m^2)$ of MoS_2 sheets drop-cast on the HOPG substrate. Inset: height profile of MoS_2 sheet consistent with a single monolayer (~ 0.8 nm), b) step edge of MoS_2 monolayer $(15 \times 15\ nm^2)$. (All STM images were acquired at V_{bias} = 300 mV, I_t = 0.1 nA).

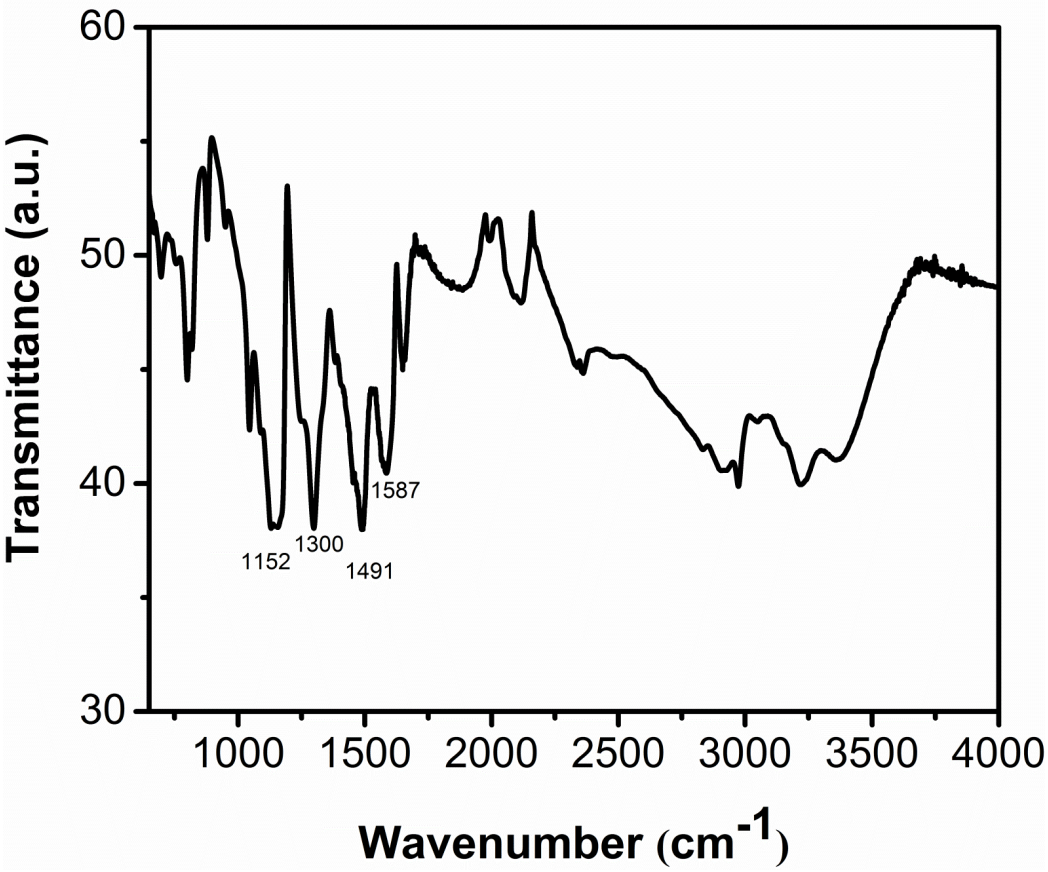

Figure S3. Attenuated total reflection (ATR) infrared spectroscopy of the PANI. The characteristic bands of polyaniline appear at 1581, 1486, 1291, and 1150 cm^{-1} which are attributed to C=C stretching modes of the quinoid, the benzenoid rings, the C–N stretching of secondary aromatic amine, and the aromatic C–H in-plane bend, respectively.[3b, 10] ATR spectra were obtained by a Nicolet iS5 FT-IR.

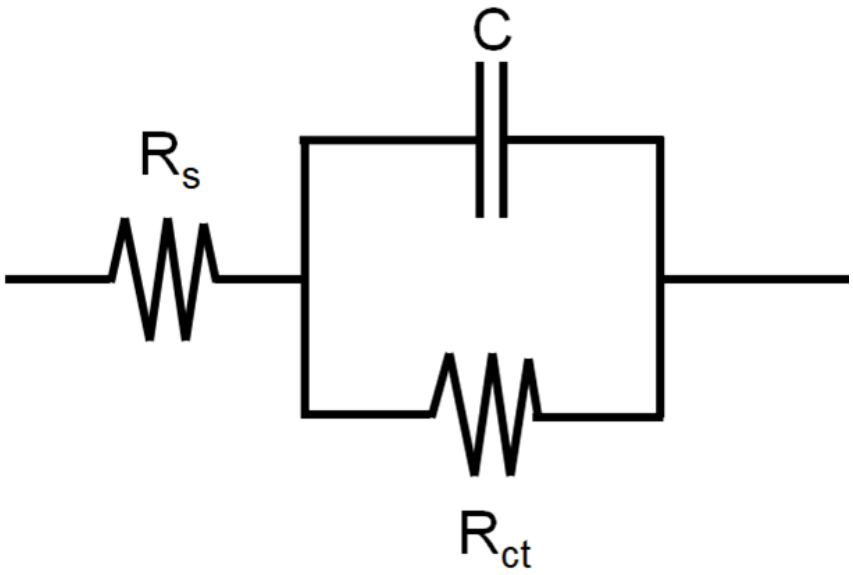

Figure S4. The equivalent circuit for the analysis for the impedance spectroscopy. R_{ct} represents the charge transfer resistance

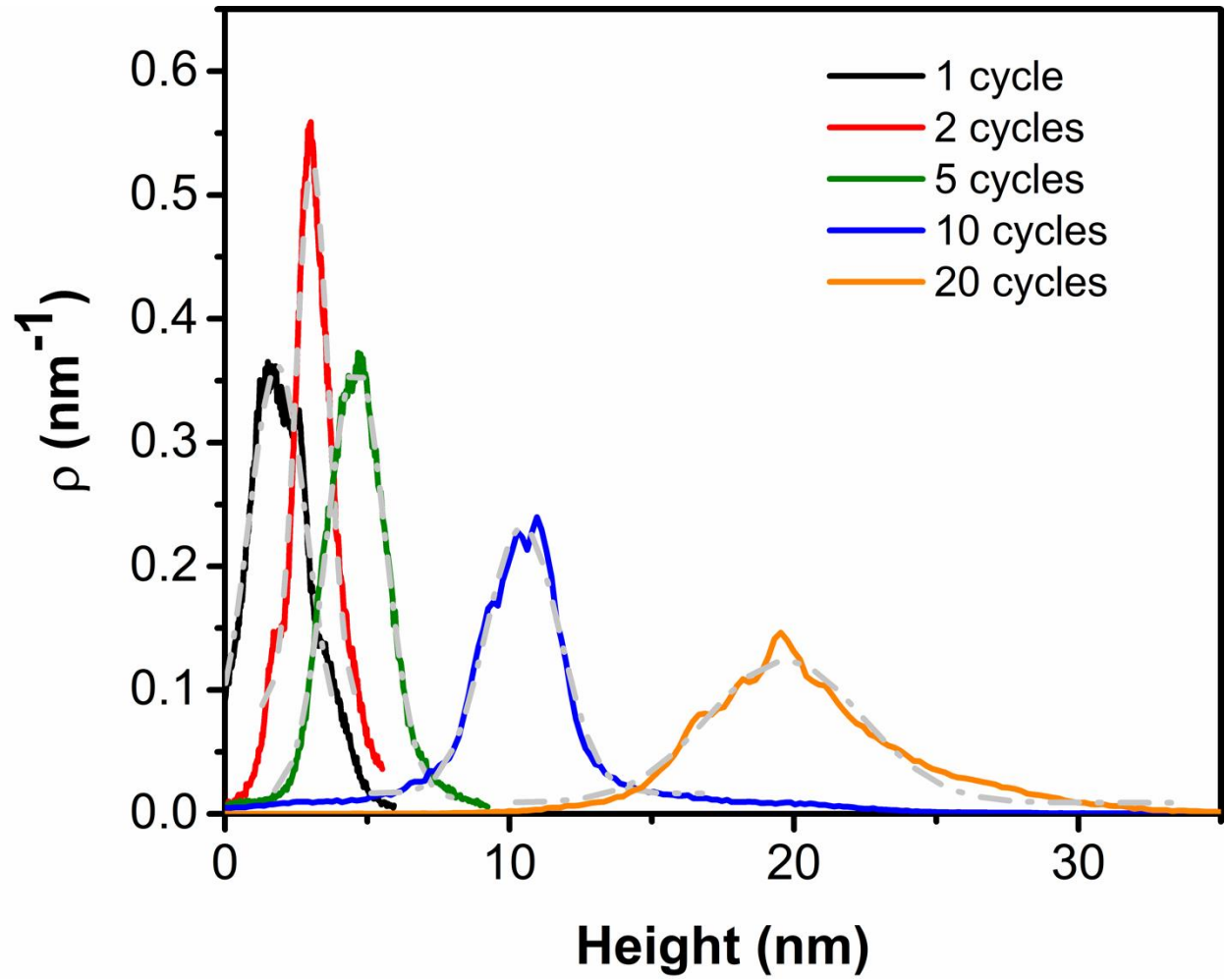

Figure S5. Height distribution functions and Gaussian fits (gray lines) obtained from the AFM images, a) 1 cycle, b) 2 cycles, c) 5 cycles, d) 10 cycles, e) 20 cycles. The AFM images were analyzed using statistical tools in Gwyddion software.

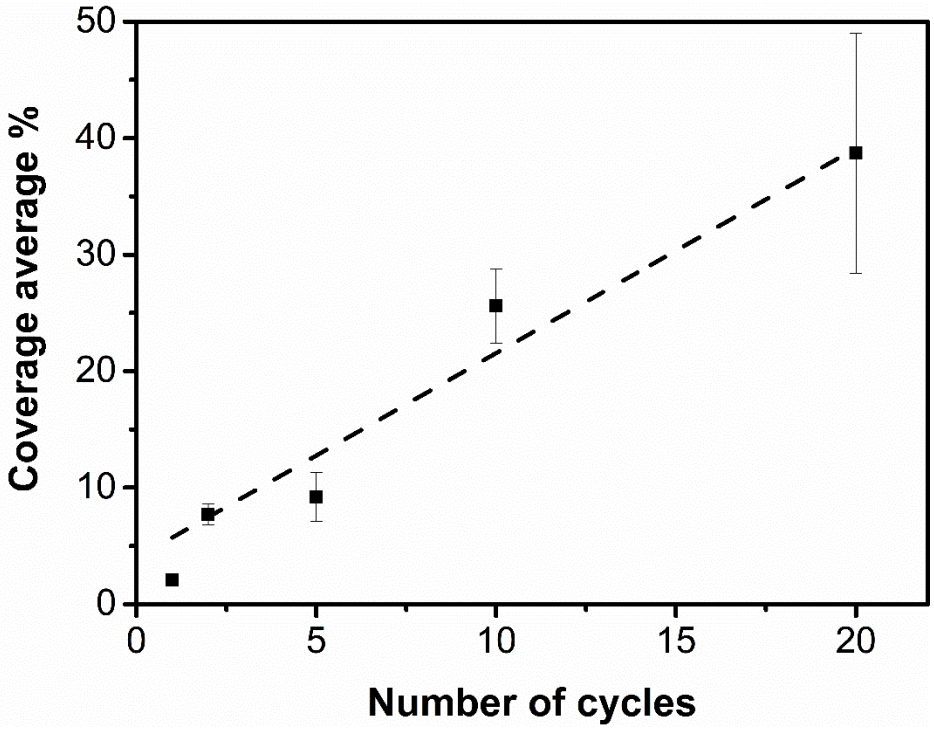

Figure S6. The surface coverage of MoS_2 sheets as a function of the number of deposition cycles obtained from the AFM images

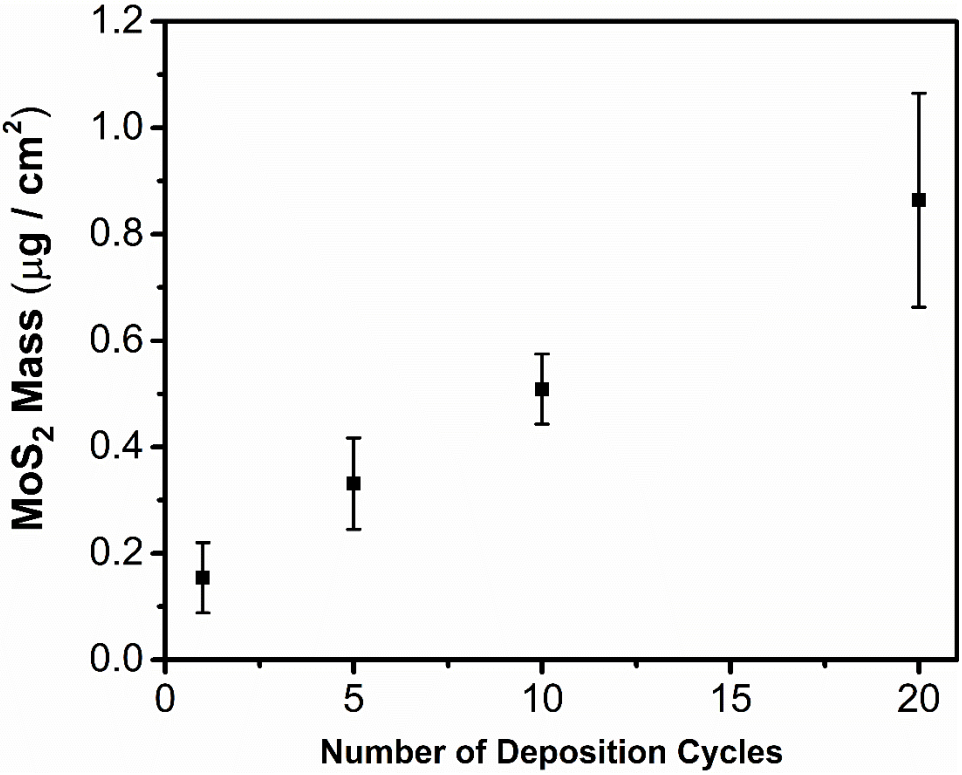

Figure S7. MoS_2 mass loading as a function of the number of deposition cycles determined by ICP-MS.

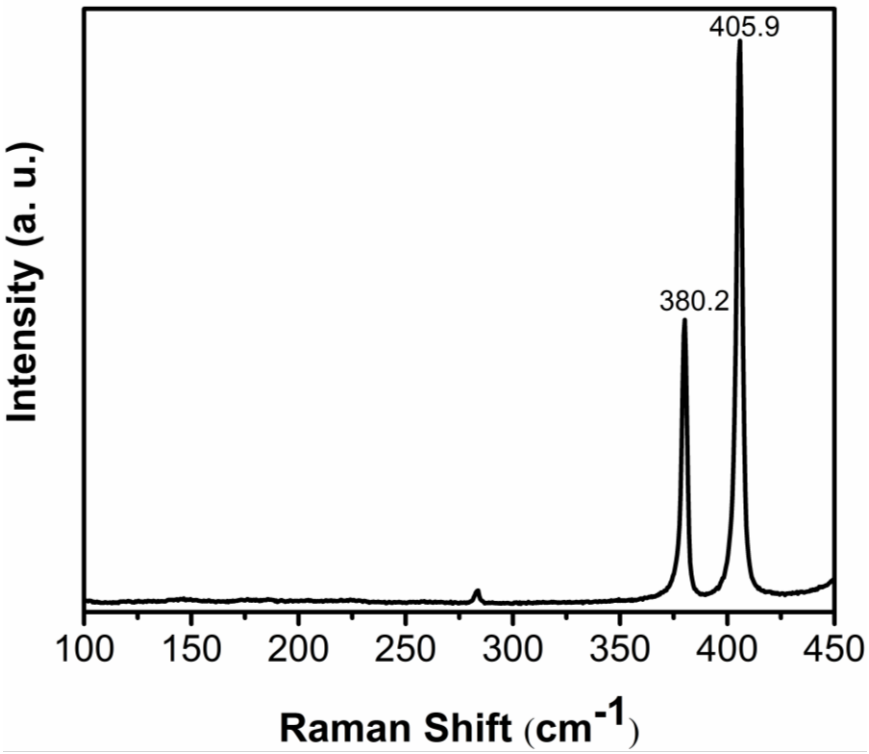

Figure S8. Raman spectra of bulk 2H-MoS_2 before exfoliation. E^1_{2g} and A_{1g} peaks appeared at 380.2 and 405.9 cm^{-1}, respectively.

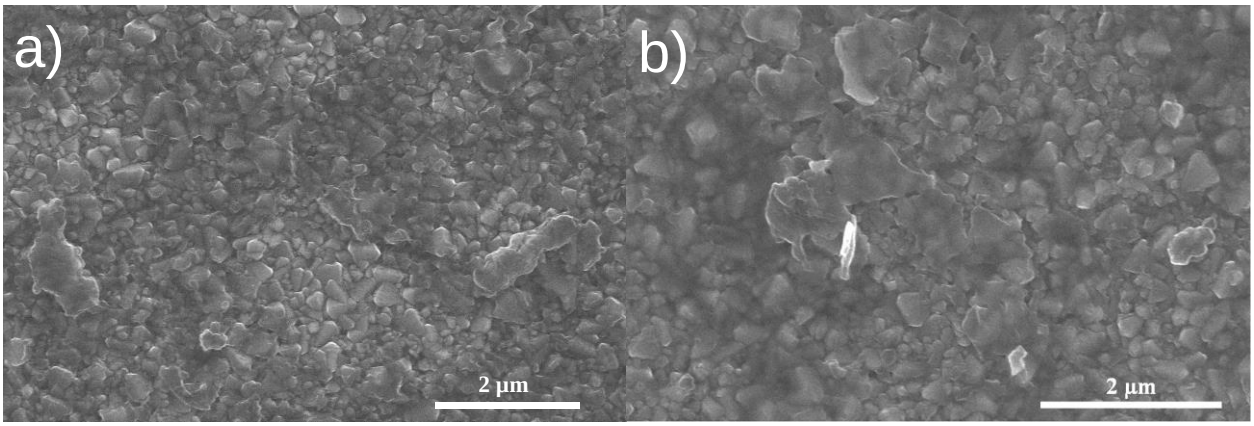

Figure S9. SEM image of assembled MoS_2 after 20 cycles deposition on FTO a) before and b) after laser treatment, confirming that the layers are intact after the laser-induced phase transition.

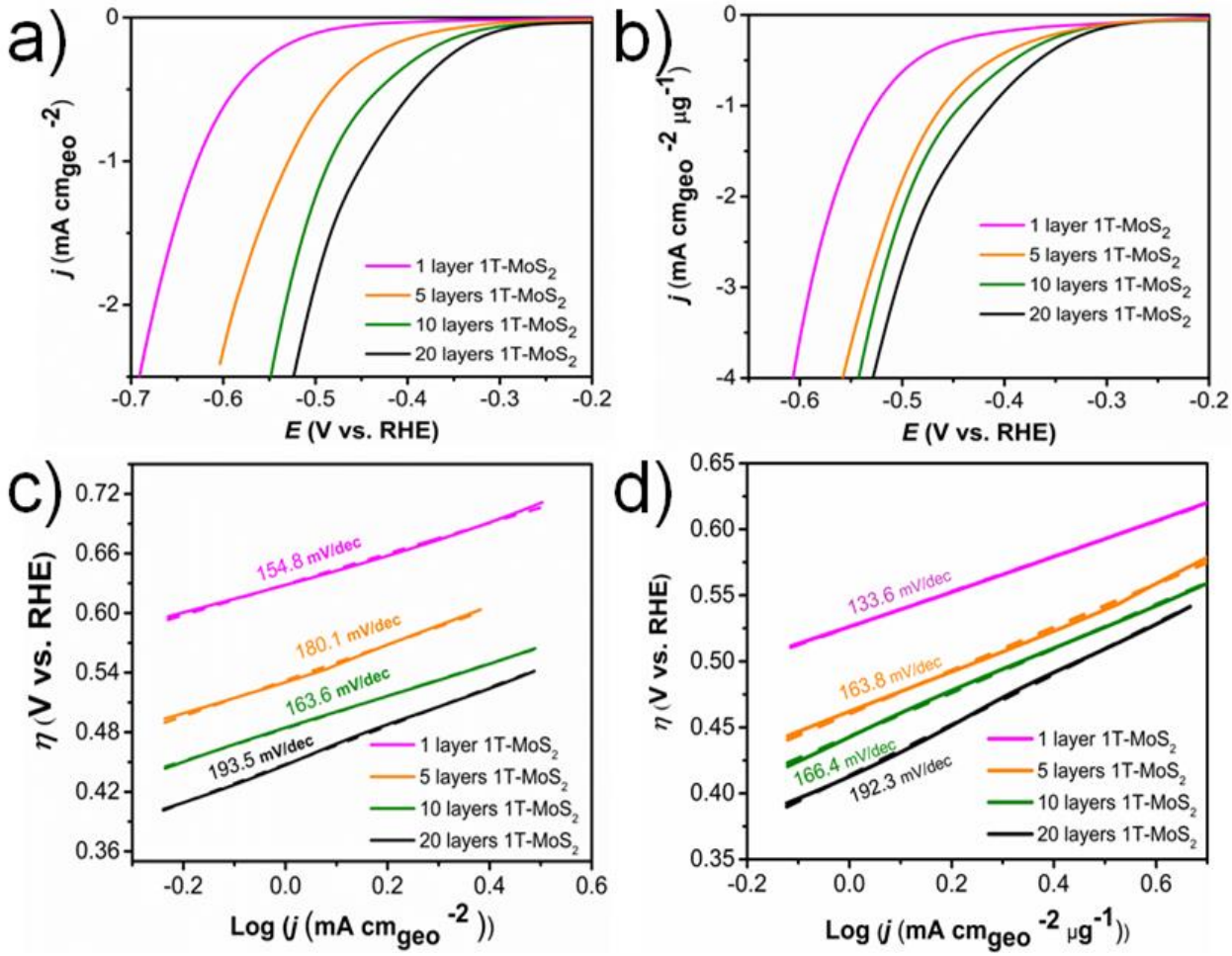

Figure S10. Polarization curves of 1T'-MoS_2 layers assembled on FTO for HER (The potential sweep rate was 10 mV s^{-1}). a) normalized to the geometric surface area, b) normalized to geometric surface area and mass; Tafel plots of the corresponding catalyst, c) normalized to the geometric surface area, d) normalized to geometric surface area and mass.

References:

[1] M. A. Lukowski, A. S. Daniel, F. Meng, A. Forticaux, L. Li, S. Jin, *J. Am. Chem. Soc.* **2013**, *135*, 10274-10277.

[2] a) E. Ahn, T. Lee, M. Gu, M. Park, S. H. Min, B.-S. Kim, *Chem. Mater.* **2016**, *29*, 69-79; b) M. G. Kanatzidis, R. Bissessur, D. C. Degroot, J. L. Schindler, C. R. Kannewurf, *Chem. Mater.* **1993**, *5*, 595-596.

[3] a) M. M. Ayad, W. A. Amer, M. Whdan, *J. Appl. Polym. Sci.* **2012**, *125*, 2695-2700; b) A. Yasuda, T. Shimidzu, *Polym. J.* **1993**, *25*, 329-338; c) M. M. Ayad, M. Whdan, *Colloid J.* **2008**, *70*, 549-554.

[4] a) A. C. Thenuwara, S. L. Shumlas, N. H. Attanayake, E. B. Cerkez, I. G. McKendry, L. Frazer, E. Borguet, Q. Kang, M. J. Zdilla, J. Sun, D. R. Strongin, *Langmuir* **2015**, *31*, 12807-12813; b) I. G. McKendry, A. C. Thenuwara, S. L. Shumlas, H. Peng, Y. V. Aulin, P. R. Chinnam, E. Borguet, D. R. Strongin, M. J. Zdilla, *Inorg. Chem.* **2018**, *57*, 557-564.

[5] D. Nečas, P. Klapetek, *Cent. Eur. J. Phys.* **2012**, *10*, 181-188.

[6] a) D. Voiry, M. Salehi, R. Silva, T. Fujita, M. W. Chen, T. Asefa, V. B. Shenoy, G. Eda, M. Chhowalla, *Nano Lett.* **2013**, *13*, 6222-6227; b) G. Eda, H. Yamaguchi, D. Voiry, T. Fujita, M. Chen, M. Chhowalla, *Nano Lett.* **2011**, *11*, 5111-5116.

[7] F. Wypych, T. Weber, R. Prins, *Chem. Mater.* **1998**, *10*, 723-727.

[8] L. Sun, X. Yan, J. Zheng, H. Yu, Z. Lu, S. Gao, L. Liu, X. Pan, D. Wang, Z. Wang, P. Wang, L. Jiao, *Nano Lett.* **2018**, *18*, 3435-3440.

[9] C. I. Lu, C. J. Butler, J. K. Huang, C. R. Hsing, H. H. Yang, Y. H. Chu, C. H. Luo, Y. C. Sun, S. H. Hsu, K. H. O. Yang, C. M. Wei, L. J. Li, M. T. Lin, *Appl. Phys. Lett.* **2015**, *106*, 1-4.

[10] M. Trchová, Z. Morávková, M. Bláha, J. Stejskal, *Electrochim. Acta* **2014**, *122*, 28-38.